Dual-drug loaded separable microneedles for efficient rheumatoid arthritis therapy

Mengchen An[a,b,c], Mengxiao Shi [a,b,c], Jingjing Su [a,b,c], Yueru Wei [a,b,c], Rongrong Luo[a,b,c], Pengchao Sun[a,b,c,*], Yongxing Zhao[a,b,c,*]

[a]Department of Pharmaceutics, School of Pharmaceutical Sciences, Zhengzhou University, No.100 Science Ave, Zhengzhou 450001, PR China

[b]Key Laboratory of Targeting Therapy and Diagnosis for Critical Diseases, Zhengzhou University, No.100 Science Ave, Zhengzhou 450001, PR China

[c]Key Laboratory of Advanced Pharmaceutical Technology, Ministry of Education of China, Zhengzhou University, Zhengzhou 450001, PR China

[*]These are corresponding authors. Address: Department of Pharmaceutics, School of Pharmaceutical Sciences, Zhengzhou University, No.100 Kexue Ave, Zhengzhou 450001, PR China; Emails: pengchao_sun@zzu.edu.cn, zhaoyx@zzu.edu.cn

Supplementary materials

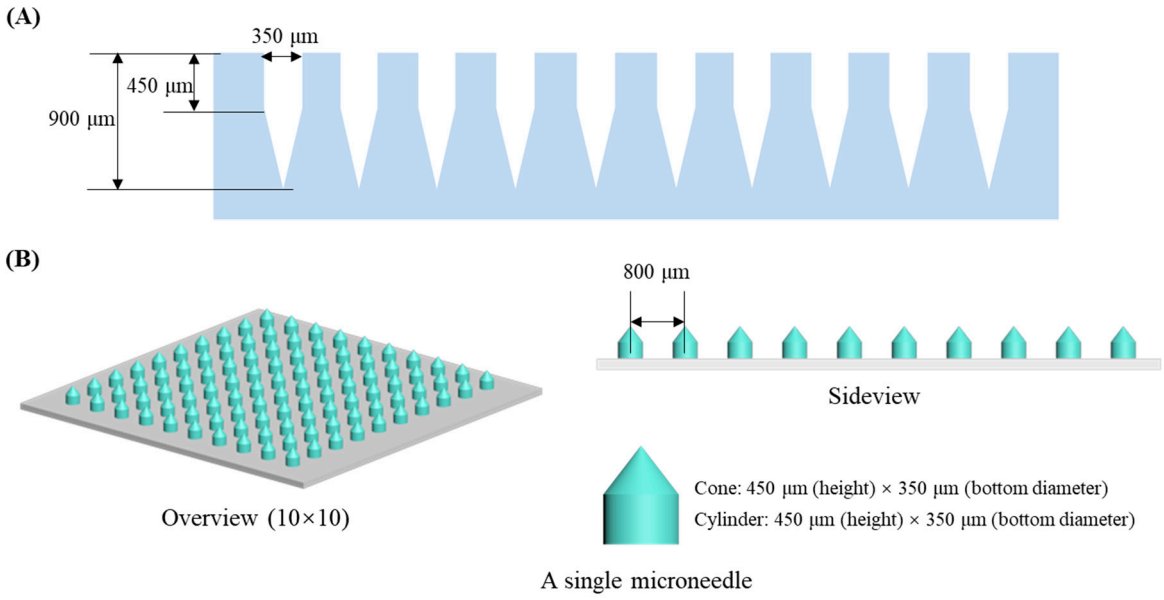

Figure S1 Overview of the designed MN. (A) Side view of the PDMS mold. (B) Master mold.

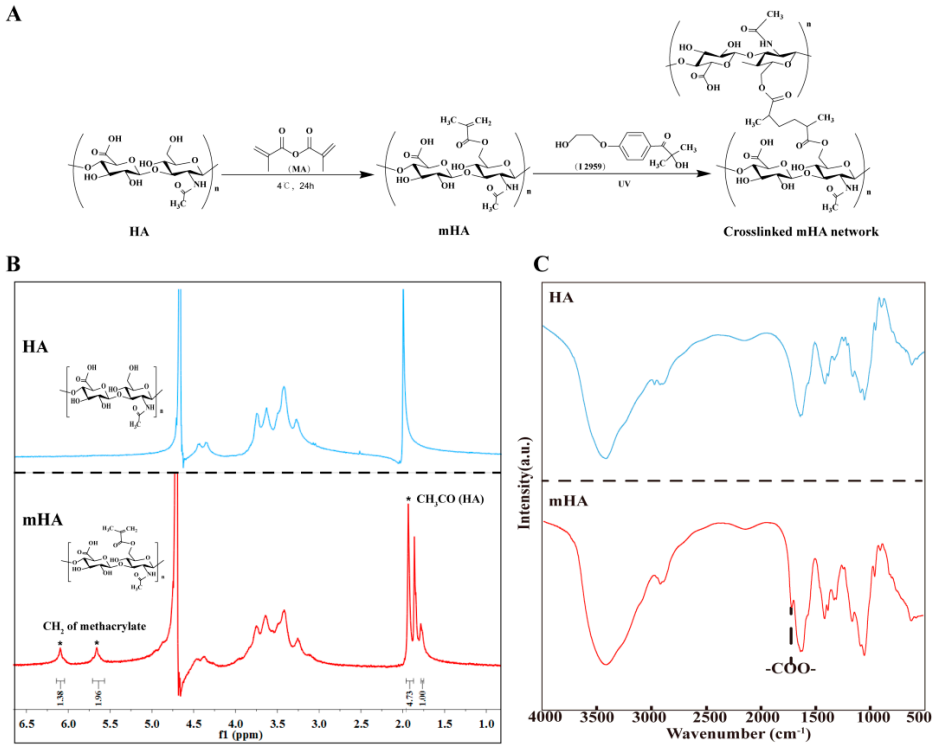

Figure S2 Synthesis and characterization of methacrylate modified hyaluronic acid (mHA). (A) Synthesis of mHA and UV initiated crosslinking. (B) ^{1}H-NMR spectra of HA and mHA.

(C) FTIR spectra of HA and mHA.

HA gained carbon-carbon double bonds after esterification with methacrylate anhydride, which leads to the cross-linking of the network after UV irradiation. The characteristic peaks at ~6.1 ppm and ~5.7 ppm represented the methacrylate protons, while the peak at ~1.9 ppm represented methyl proton signals of HA, indicating the successful preparation of mHA (Figure S2B). The successful synthesis of mHA was further verified by FTIR with a characteristic absorption at ~1700 cm^{-1} (Figure S2C).

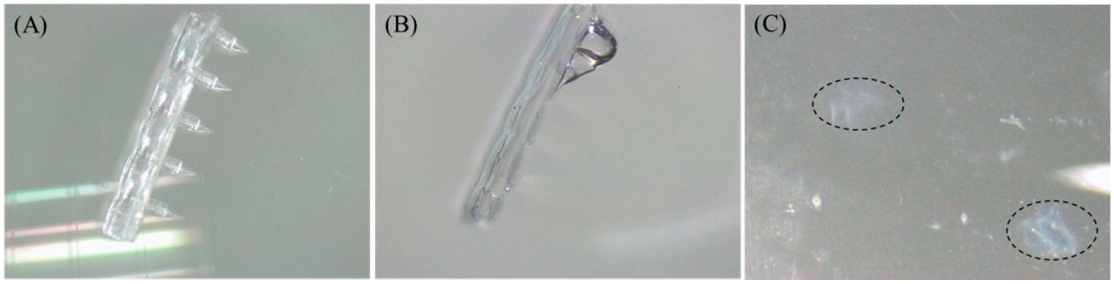

Figure S3 The separation of MN. (A) Before water rinse. (B) Dissolution of the needle body. (C) Separated needle tips.

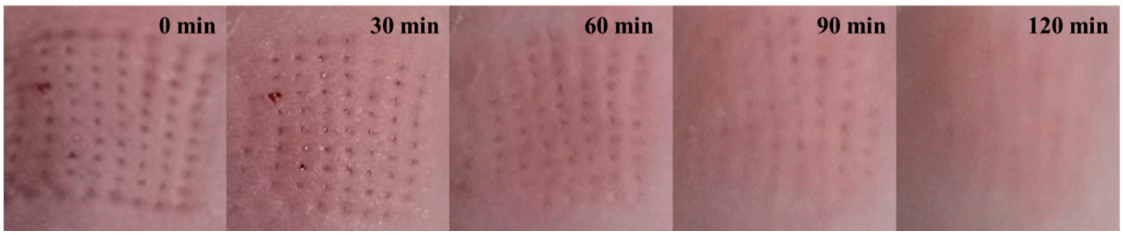

Figure S4 Skin recovery after application of mHA prepared MN.

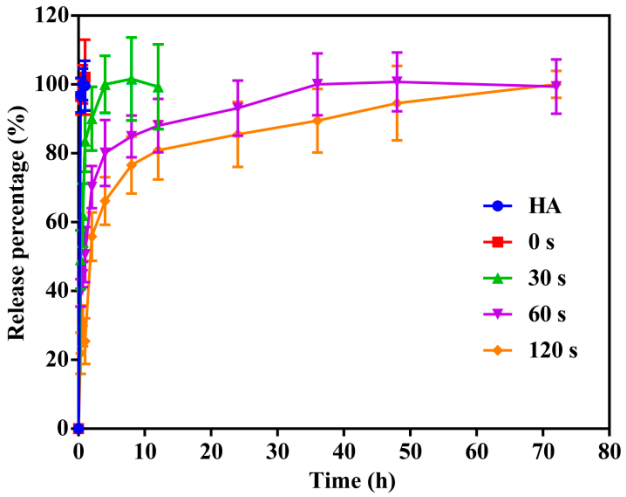

Figure S5 *In vitro* release of BSA-FITC from the needle tips of the separable MN (0~80 h).

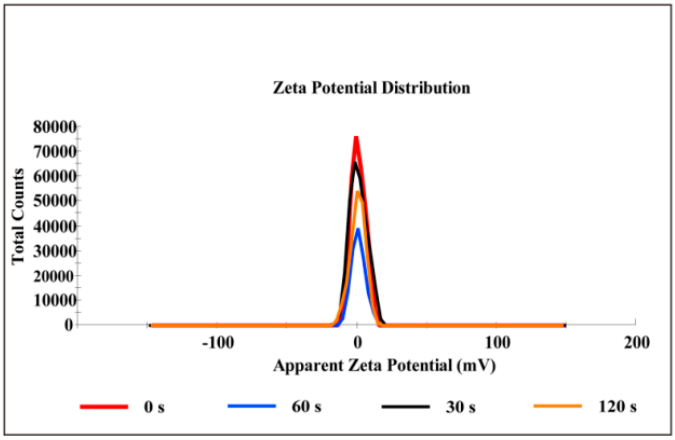

Figure S6 Zeta potential of TCZ after UV irradiation.

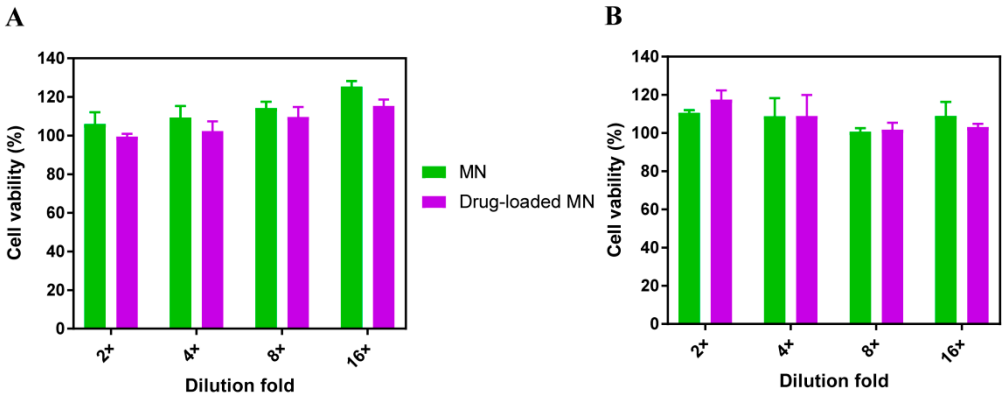

Figure S7 The cytotoxicity of MN and drug-loaded MN against murine fibroblasts L929 (A) and human fibroblasts FLS (B).

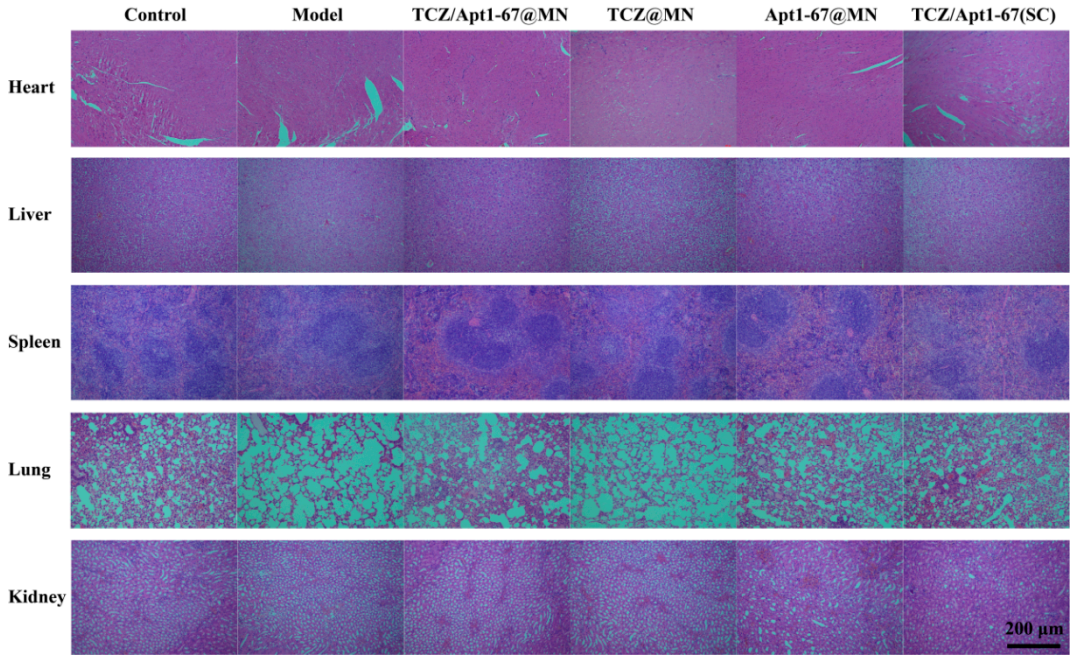

Figure S8 Influences of various treatments on the organs of mice.

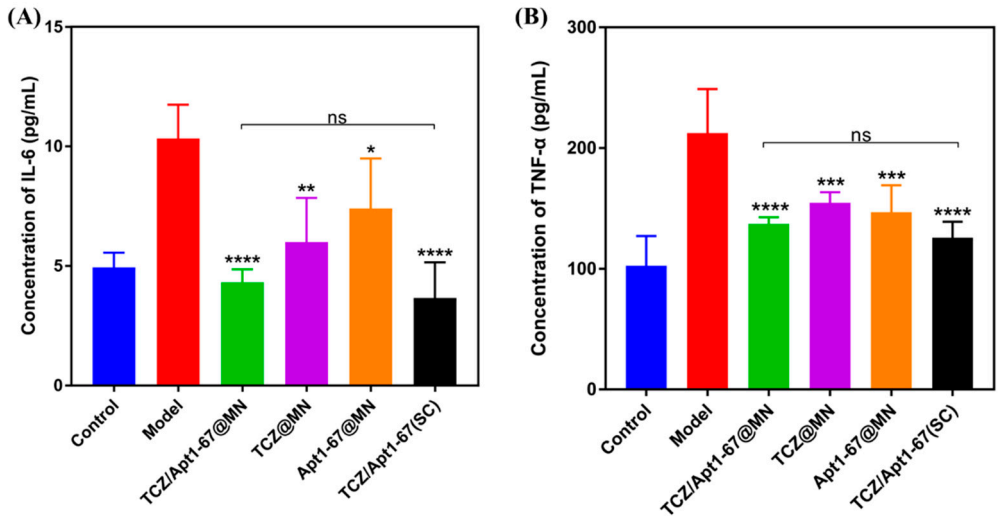

Figure S9 Serum levels of IL6 (A) and TNF-α (B). *p＜0.05,**p＜0.01, ***p＜0.001， ****p＜0.0001, ns: not significant